Understanding hydrogen evolution reaction in bicarbonate buffer

Marcandalli, G.; Boterman, K.; Koper, M.T.M.

Journal of Catalysis 405 (2022) 346–354

Contents lists available at ScienceDirect

Journal of Catalysis

journal homepage: www.elsevier.com/locate/jcat

Understanding hydrogen evolution reaction in bicarbonate buffer

Giulia Marcandalli, Katinka Boterman, Marc T.M. Koper *

Leiden Institute of Chemistry, Leiden University, PO Box 9502, 2300 RA Leiden, the Netherlands

ARTICLE INFO

Article history:
Received 29 September 2021
Revised 10 November 2021
Accepted 13 December 2021
Available online 18 December 2021

Keywords:
Hydrogen evolution
Gold electrode
Platinum electrode
Bicarbonate reduction
Cation effects

ABSTRACT

Buffers are often employed as electrolytes for their ability to resist to pH changes. Still, they are not just spectators in the electrocatalytic processes, rather they may take a primary role. Here, we attempt to understand the mechanism of the hydrogen evolution reaction (HER) in bicarbonate-containing electrolytes on two distinct materials, Au and Pt. Keeping the bulk pH constant, voltammetric measurements reveal a promotional effect on the HER rate in the presence of bicarbonate buffer, as well as a substantial change in the reaction mechanism with a Tafel Slope in bicarbonate resembling the one in acidic media (ca. 100 and 40 mVdec^{-1} on Au and Pt, respectively). Nevertheless, because of the increase in surface pH due to the concomitant water reduction ($2H_2O + 2e^- \rightarrow H_2 + 2\ OH^-$), bicarbonate is consumed by acid-base reactions and the bicarbonate branch of HER becomes significant only in the presence of large bulk buffer concentrations. Bicarbonate and water reduction appear intrinsically different, as they exhibit opposite dependence on the cation identity and scale differently with the specific area of the electrode. Through microkinetic modelling, we exclude that HER in bicarbonate can be explained via the generation of a proton by solution acid-base reactions. Rather, we suggest a direct bicarbonate reduction pathway, which, due to the negatively charged reactant, is strongly dependent on the cation concentration.

1. Introduction

The electrochemical production of hydrogen from water holds the promise to be a commercially competitive way to synthesize renewable fuel. On the other hand, when optimizing a different electroreduction pathway, the hydrogen evolution reaction (HER) becomes an unwanted process, which limits the energy output of the desired reaction. A representative case for the latter is the CO_2 electrochemical reduction (CO2RR), where the competitive HER co-determines the Faradaic Efficiency (FE) to CO2RR [1,2]. To identify strategies to limit the HER, it is crucial to determine the proton source leading to HER. Traditionally, HER has been extensively studied in acidic solutions, where the hydronium ion is the proton source. Hydronium (most commonly referred as proton) reduction is characterized by a fast kinetics, and is mainly constrained by mass transport [3]. By contrast, for increasing pH, where water is the main proton donor for HER (Eq. 1), the reaction rate is hindered by more sluggish kinetics [4].

$$2H_2O + 2e^- \rightleftharpoons H_2 + 2OH^- \quad (1)$$

Water dissociation to release hydrogen is generally considered to have a higher barrier than hydrogen evolution in acidic media. While HER from hydronium is roughly independent of the electrolyte nature, HER from water exhibits a strong dependence on the composition of the electrified interface. The surface cation concentration [4], as well as the nature of the cation [5], determines the rate of water reduction by interacting with the transition state of the water dissociation step. Still, hydronium and water are not the only proton sources. In general, every weak acid contained in the electrolyte may be considered as a viable proton donor. Specifically, buffering electrolytes species may be regarded not only as pH regulators, but also as possible proton donors, once the surface pH equals the pK_a of the buffering couple [3,6]. This is the case of the widely employed bicarbonate electrolytes for CO2RR studies, which act as proton donor (PD) for HER (Eq. 2), limiting the FE of CO2RR to CO [2].

$$2HCO_3^- + 2e^- \rightleftharpoons H_2 + 2CO_3^{2-} \quad (2)$$

The phosphate buffer $H_2PO_4^-/HPO_4^{2-}$, having a neutral pK_a of 7.1, is also widely employed in electrochemistry, as well as in biological systems. Studying HER in phosphate electrolytes (pH ca. 7) on platinum, Obata et al. proposed that the mechanism of HER involves a solution acid-base reaction between phosphate and water to release an hydronium ion, followed by hydronium reduction to generate H_2 [3]. Assuming faster kinetics of the solution homogeneous reactions compared to the experimental ones, digital simulations based on the proposed mechanism could reproduce with good agreement

* Corresponding author.
E-mail address: m.koper@chem.leidenuniv.nl (M.T.M. Koper).

https://doi.org/10.1016/j.jcat.2021.12.012
0021-9517/

the experimental HER currents. On the other hand, studying the HER in phosphate buffers on gold, Jackson et al. suggested that the phosphate species forms a surface complex prior to hydrogen discharge [6]. This hypothesis was supported by a previous study indicating that in acetonitrile the steric hindrance of the electrolyte conjugated acid also plays a role in dictating the kinetics of the HER process [7]. Nonetheless, switching to an aqueous medium, the steric hindrance of the PD was not a crucial factor in determining HER activity [7].

Motivated by our recent results on electrolyte effects during CO_2 reduction [2], we investigated in more detail the mechanism of HER in bicarbonate electrolytes. We probed whether the bicarbonate provides the proton donor I) through its solution acid-base reaction liberating an hydronium ion, which undergoes reduction or II) through the formation of a (cation)-anion surface complex at the electrified interface resulting in the hydrogen discharge, as drawn in Fig. 1. We combined voltammetry measurements under forced-convection on a gold and on a platinum rotating disk electrodes (RDE) as a function of the pH and buffer nature, bicarbonate buffer concentration, cation identity, cation concentration and electrode roughness. We rationalized the dependence of the total HER current on the electrolytes parameters, in terms of the separate contributions of bicarbonate-mediated-reduction and water reduction. Finally, with the help of a microkinetic model, we discuss the mechanism that better describes bicarbonate reduction.

2. Experimental

2.1. Chemicals and Materials

Electrolytes were prepared from H_2SO_4 (96 %, Merck Suprapur™), $HClO_4$ (70 %, Merck Suprapur™), $KHCO_3$ (Emsure™ACS Merck), K_2CO_3 (99.995 % trace metals basis, Sigma–Aldrich), $KClO_4$ (Emsure™ACS Merck), $NaHCO_3$ (Emsure™ACS Merck), Na_2CO_3 (99.999 %, Merck Suprapur™), $NaClO_4$ (Emsure™ACS Merck), NaH_2PO_4 (Emsure™ACS Merck), Na_2HPO_4 (99.99 %, Merck Suprapur™), Li_2CO_3 (99.999 % trace metals basis, Acros organics), $LiOH{\bullet}H_2O$ (99.995 % trace metals basis, Alfa Aesar), NaOH (30 % Suprapure, Merck), KCl (Emsure, Merck) and Milli-Q water (resistivity $\geqslant$18.2 MΩ cm). Before experiments, the electrolytes were purged for ca. 20 min with Ar (6.0 purity, Linde) to remove any dissolved oxygen. After Ar purging, the pH of the given electrolyte was determined with a pH meter (SI Analytics Lab 855 Benchtop Meter). The measurements were performed using a Bio-Logic VSP300 potentiostat and a Modulated Speed Rotator (Pine Research Instrumentation). The glassware was stored overnight in a 1 g L^{-1} $KMnO_4$ solution. Then, $KMnO_4$ was removed by adding a dilute H_2O_2 solution, acidified with a few drops of H_2SO_4 and the glassware was boiled 5 times in MilliQ water.

2.2. Experimental Procedure

The electrochemical experiments were performed at room temperature in two three-electrode configuration cells. Both cells contained a home-made reversible hydrogen electrode (RHE) as reference electrode and a gold wire (99.99 % purity) as counter electrode. Unless otherwise stated, all the potentials are reported on the RHE scale. The working electrode, a gold disk (ø = 5.0 mm, Pine Research Instrumentation), was mechanically polished with diamond suspension of decreasing particle size (3, 1, 0.25 μm). Next, the Au disk was sonicated in a mixture of MilliQ water and acetone for ca. 10 min. In the first cell containing 0.1 M H_2SO_4, we performed the electrochemical characterization of the gold disk by cyclic voltammetry (CV) from 0.1 to 1.75 V at 50 mVs^{-1} (see Figure S1 in the Supporting Information). Then, in the second cell the catalytic activity for HER was measured by CVs between 0.1 and −1.2 V vs RHE in the given electrolyte at 10 mVs^{-1} and 2500 RPM. The CVs were compensated for 85% of the Ohmic drop, as measured by Electrochemical Impedance Spectroscopy (EIS) at 0.1 V. In between each CV in the HER region, we assessed the quality of the electrode surface by measuring a CV between 0.1 and 1.65 V. The total current measured during the cathodic scan is attributed to HER, as we did not detect any oxidation charge associated with the bicarbonate reduction to C_1 molecules [8] (see Figure S3 in the Supporting Information). The electrochemically active surface area (ECSA) of the Au disk was determined by integrating the reduction peak of the gold oxide in 0.1 M H_2SO_4 and dividing it by the charge corresponding to a Au monolayer (390 μCcm^{-2}). Hence, we normalized the current for the ECSA. Each measurement was repeated three times and the average HER current was used to calculate the reaction order in bicarbonate and the dependence on the cation nature.

The measurements performed with a Pt disk (ø = 5.0 mm, Pine Research Instrumentation) as the working electrode followed the same procedure reported above except for a few differences. Namely, a Pt (99.99 % purity) counter electrode was used, the characterisation CV was measured between 0.05 and 1.5 V (see Figure S1 in the Supporting Information), the Ohmic drop was measured at 0.5 V and the HER current was measured between 0.1 and −0.4 V. The ECSA of the Pt disk was determined by calculating the charge of the hydrogen adsorption region and dividing it by the charge corresponding to a monolayer of adsorbed hydrogen (230 μCcm^{-2}).

To study the dependence of the HER current on the ECSA, we roughened the Au RDE by performing several cycles of oxidation (5 s at 1.2 V *vs.*AgAgCl) and reduction (20 s at −0.4 V *vs.*AgAgCl) in 0.5 M KCl. Then, as previously described, we determined the ECSA by electrochemical characterization in 0.1 M H_2SO_4 (see Fig. S2 in the Supporting Information). The roughness factor was calculated dividing the ECSA by the geometrical area (0.1963 cm^{-2}). The value of the ECSA was stable over the course

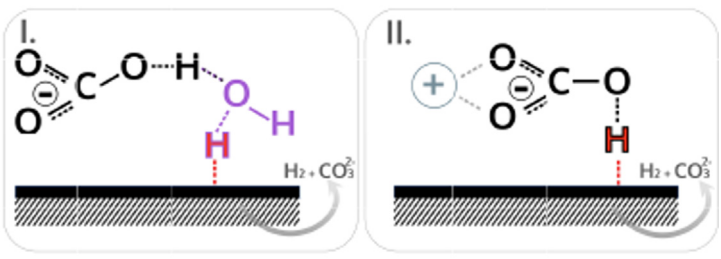

Fig. 1. Schematics of the two possible mechanisms for HER in bicarbonate electrolytes.

of the measurement, as established by comparing the area of the gold oxide reduction peak at the beginning, and at the end of the measurement.

2.3. Microkinetic Model

To quantify the HER current in bicarbonate solutions following model I, where bicarbonate acts as a "shuttle" of proton to the surface through solution acid-base reactions, we constructed a microkinetic model. Model II would require additional parameters, such as the thermodynamics and kinetics of the adsorption of the cation–anion complex, which have not been reported. The simulation consists of a system of partial differential equations (PDEs), one for each species (i) we want to model, expressing the concentration (c_i) as a function of time (t) and space (x). The PDE models the mass transport, in terms of diffusion and convection (migration is reasonably neglected at this electrolyte ionic strength of 3 M), and the effect of the homogeneous reactions (R_i) according to:

$$\frac{\partial c_i}{\partial t} = D_i \frac{\partial^2 c_i}{\partial x^2} - v\frac{\partial c_i}{\partial x} + R_i, \tag{3}$$

where c_i (mol dm^{-3}) is the concentration, D_i (m^2 s^{-1}) is the diffusion coefficient and v (m s^{-1}) is the convective velocity. We modelled the variation in c_i for OH^-, H^+, CO_3^{2-} and HCO_3^-. Given the large concentration of water in aqueous solution, we consider its concentration to be constant also in the diffusion layer. The diffusion term is expressed by Fick's law [9]. The convective velocity (v) is expressed as a function of the rotation speed across the distance (x) from the surface (x = 0) as:

$$v = -0.51\omega^{1/2}\nu^{-1/2}x^2, \tag{4}$$

where ω (rad s^{-1}) is the rotation speed frequency, ν (m^{2}s^{-1}) is the kinematic viscosity of the solution and x (m) is the distance from the electrode surface. The homogeneous reactions included in the models are the self-ionization of water (Eq. 5) and and the acid-base reactions of the bicarbonate buffer (Eq. 6 and 7).

$$H_2O \rightleftharpoons H^+ + OH^-, \tag{5}$$

$$HCO_3^- + OH^- \rightleftharpoons CO_3^{2-} + H_2O, \tag{6}$$

$$HCO_3^- \rightleftharpoons CO_3^{2-} + H^+. \tag{7}$$

To estimate the effect of the solution reactions kinetics on the HER current, besides using the reported homogeneous reaction rate constants (see Table S1 in the Supporting Information), we also run simulations with a fictitious rate constant for reaction (7). The system of PDEs was solved for given initial conditions (*at t = 0*, c_i=$c_{i,bulk}$) and boundary conditions. At the diffusion layer/bulk (right) boundary, we set that $c_{i,right} = c_{i,bulk}$. At the diffusion layer/electrode (left) boundary, the flux of i is equal to the rate at which i is consumed/produced by the electrochemical reaction. According to model I, where only protons are consumed by the electrochemical reaction, we can write the following boundary conditions:

$$D_{OH^-}\frac{\partial c_{OH^-}}{\partial x} = 0, \tag{8}$$

$$D_{H^+}\frac{\partial c_{H^+}}{\partial x} = -\frac{2 * j_I}{nF}, \tag{9}$$

$$D_{HCO_3^-}\frac{\partial c_{HCO_3^-}}{\partial x} = 0, \tag{10}$$

$$D_{CO_3^{2-}}\frac{\partial c_{CO_3^{2-}}}{\partial x} = 0. \tag{11}$$

The current for HER according to model I is written in a Butler–Volmer form, considering that for Au electrode the rate determining step is the Volmer step [10], according to:

$$j_I = nFk^0 c_{H^+,s} exp\left[\frac{\alpha nF}{RT}(E - E^0)\right], \tag{12}$$

where n the number of electron transferred is 2, $c_{H^+,s}$ is the surface concentration of H^+, k^0 the reaction rate is 1.0 $*$ 10^{-6} m s^{-1}, α the transfer coefficient is 0.5 and E^0 the H_2/H^+ standard equilibrium potential is 0.0 V vs. RHE. The numerical simulations were performed using the kinetics data (k^0 and α) reported in the literature for proton reduction on Au [11]. Since on Au HER takes place far from the standard equilibrium potential, at the operating potentials we can neglect the contribution of hydrogen oxidation reaction. The system of PDEs was solved with MATLAB R2020 over a spacemesh x large enough to contain the diffusion layer (x=$10^{-4.75}$ m at 2500 RPM).

3. Results

3.1. Electrochemical Measurements

In Fig. 2, the voltammograms for HER on (A) Au and (B) Pt are shown in acidic solution (pH 0.0), in phosphate (pH 7), in bicarbonate (pH 9.7) and in alkaline media (pH 9.7). Throughout the paper, all the voltammograms are measured at 10 mVs^{-1} and 2500 RPM, unless otherwise stated. It is well known that HER depends on the pH, as the proton source switches from hydronium ion in acidic pH to water in alkaline conditions. The different nature of the proton donor explains the shift in the onset potential of HER observed even on a RHE scale at pH 0.0 (-0.1 V for Au and 0.08 V for Pt) compared to pH 9.7 (-0.9 V for Au and −0.02 V for Pt) for both electrode surfaces in a solution of $NaClO_4$. Addition of a buffer at neutral (phosphate) and mildly alkaline (bicarbonate) pH results in an intermediate onset potential for HER [-0.25 (0.05) V phosphate and −0.4 (0.03) V bicarbonate on Au (Pt)], between the onsets for proton and water reduction. On Pt, the onset potential in phosphate and bicarbonate is almost the same, while on Au a more negative applied potential is required for HER in bicarbonate than in phosphate. For the same pH (9.7) and cation concentration (1.5 M Na^+), we clearly measure a higher HER current and a less negative onset potential in the presence of bicarbonate buffer compared to the solution containing $NaClO_4$. The latter observation is in agreement with our previous claim that bicarbonate acts as a proton donor in the HER [2]. We expect that as the nature of the proton donor changes, the mechanism and the kinetics of the reaction change as well. Fig. 2 displays the derived Tafel slope (TS) for HER for (C) Au and (D) Pt in the various solutions. In agreement with previously reported values, in acidic media we measured a values for the TS of 100 mVdec^{-1} on Au [10] and 40 mVdec^{-1} on Pt [12]. These TS values have been ascribed to a reaction mechanism involving as the rate determining step (RDS) the hydrogen adsorption (Volmer step) and the hydrogen surface recombination (Heyrovsky step) for Au and Pt, respectively [13]. On the other hand, we measured a TS of 240 mVdec^{-1} (on Au) and 120 mVdec^{-1} (on Pt) for water reduction, as this reaction is more kinetically hindered compared to proton reduction. Our values match the ones reported in the literature for water reduction with the RDS being the first electron transfer (Volmer step) [4,14], even if the interpretation of TS values on Au is still under debate [4]. In the presence of buffering species (phosphate and/or bicarbonate), we measured an initial TS of 100 and 40 mVdec^{-1}, for Au and Pt respectively. Interestingly, we measure faster HER kinetics in the presence of the buffering species, resembling the one measured for hydronium

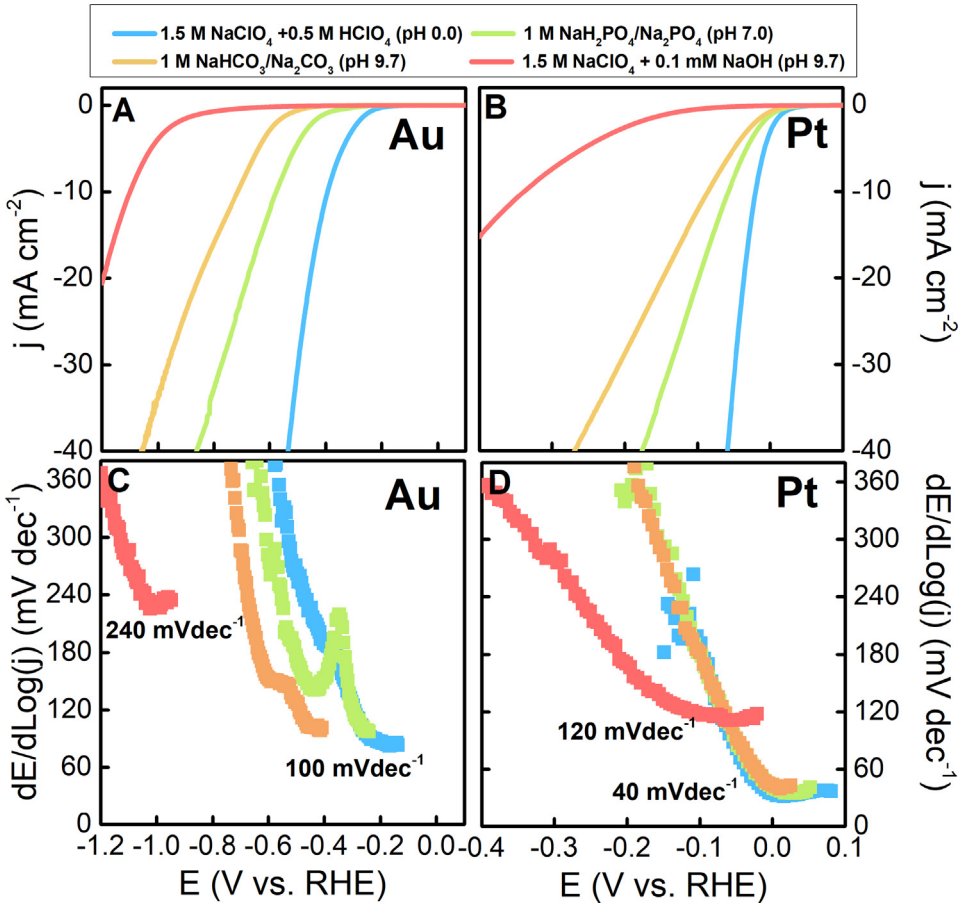

Fig. 2. Voltammetry of (A) Au and (B) Pt RDE electrode in Ar-saturated 0.5 M $HClO_4$ + 1.5 M$NaClO_4$, 1.0 M equimolar NaH_2PO_4/Na_2HPO_4, 1.0 M equimolar $NaHCO_3/Na_2CO_3$ and 0.1 mM NaOH + 1.5 M $NaClO_4$ at 10 mVs^{-1} and 2500 RPM. In all the electrolytes the Na^+ concentration is constant and equal to 1.5 M. Tafel slopes for HER in the different electrolytes for (C) Au and (D) Pt, obtained from the differentiation of voltammetry in (A) and (B), respectively.

reduction. With more negative applied potentials, on gold we noticed that in phosphate- and bicarbonate-containing electrolytes, the TS levels off around 140 $mVdec^{-1}$, after an initial increase (at −0.4 V in phosphate and at −0.55 V in bicarbonate). The reason for the potential dependence of the TS is unclear, but we may postulate that is due to the effect of the buffer in suppressing the concentration gradient developing at the electrode surface and/or to the onset of water reduction pathway promoted by the increase in surface pH.

To deepen the understanding of the HER mechanism in bicarbonate electrolytes, we studied the dependence of HER activity on the bicarbonate concentration. Importantly, the measurements were performed in equimolar solutions of bicarbonate/carbonate (as initially prepared by weight), and as a consequence the electrolyte pH corresponds to the buffer pK_a. Since no other changes in pH and/or in temperature were made, we can reasonably assume that the concentration of the species at equilibrium is comparable to the ones of the as-prepared solutions. Investigating the role of buffering species, we want to stress the importance of performing experiments in equimolar solutions of the weak acid (AH)/conjugated base (A^-) to minimize the concentration gradients generated during the electrocatalytic process. As recently reported [2,4], the cation concentration is also crucial in determining the HER activity. To assess the reaction order in AH, hence, it is fundamental to keep the cation concentration constant. Indeed, varying the concentration of AH along with the concentration of the cation leads to convolution of the effect of AH and cation concentration on the HER activity (see Fig. S4 in the Supporting Information). Fig. 3 shows the voltammograms for (A) Au and (B) Pt for different concentrations of equimolar HCO_3^-/CO_3^{2-} (at constant 1.5 M concentration of Na^+), from which the reaction order for HER in bicarbonate is extracted for (C) Au and (D) Pt. From the voltammograms, we observe that increasing the concentration of HCO_3^-/CO_3^{2-} has in general a promoting effect on the HER current. However, the reaction order gives better insights into the bicarbonate concentration dependence of HER. For both electrode surfaces, we observed two different reaction order regimes depending on the buffer concentration. For low buffer concentrations, we observe a slightly negative reaction order (-0.1) for Au and a slightly positive reaction order for Pt, i.e. 0.3 at −0.1 V decreasing to 0.1 at more negative potentials. Importantly, the concentration range for this latter regime expands to higher buffer concentrations, as the applied potential becomes more negative. On Au at less negative potential (up to −1 V), the low buffer concentration regime includes 0.002 and 0.006 M solution, while at −1.2 V the concentration range up to (and including) 0.2 M is involved. On Pt, the low buffer concentration regimes goes from 0.002 to 0.02 M, expanding to 0.066 M at the most negative applied potential (-0.4 V). In the second regime (the high buffer concentration regime), the reaction order in bicarbonate is positive for both surfaces and is slightly potential dependent. On Au, the reaction order is ca. 0.8 at less negative potential, decreasing to ca. 0.4 at more negative potential. On Pt, the reaction order is ca. 0.5 in all the studied potential range. The reaction order in bicarbonate decreases as the potential becomes more negative and water reduction starts, resulting in

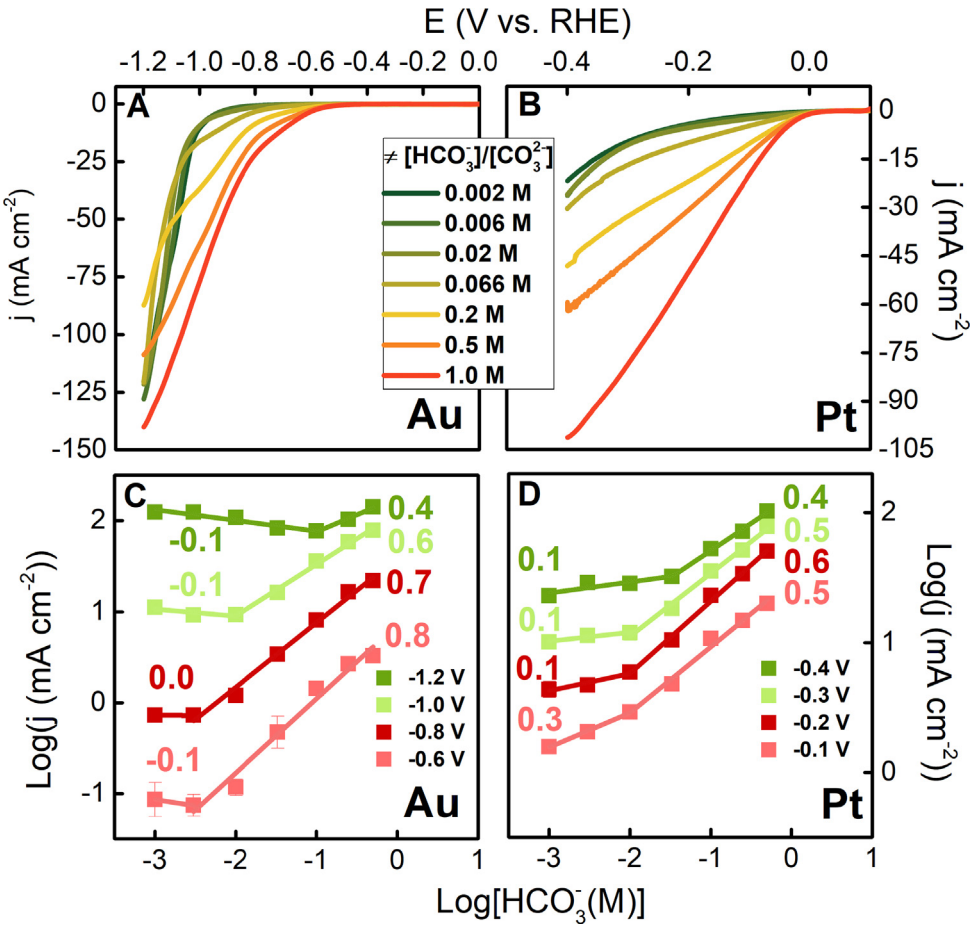

Fig. 3. Voltammetry of the (A) Au and (B) Pt RDE electrode in Ar-saturated equimolar HCO_3^-/CO_3^{2-} solution of different concentrations (0.002, 0.006, 0.02, 0.066, 0.1, 0.2, 0.5 and 1.0 M) and constant (1.5 M) concentration of Na^+ (by addition of $NaClO_4$) at 10 mVs^{-1} and 2500 RPM. Reaction order in bicarbonate for HER on (C) Au and (D) Pt as extracted from (A) and (B), respectively.

the consumption of AH to buffer the increase in the local pH. We ascribe the presence of two different regimes depending on the bicarbonate concentration, independently from the metallic surface, to the convoluted effect of bicarbonate concentration on bicarbonate and water reduction. First of all, at low buffer capacity, a large concentration gradient in bicarbonate is generated because of the increasing surface alkalinity with the current density. This increase in the surface pH leads to a depletion of bicarbonate at the surface, thus leading to a suppression of the bicarbonate branch of HER. Indeed, the low concentration buffer regime expands to higher concentrations for increasingly negative potential, as a higher buffer capacity is required to minimize pH changes. Secondly, as the changing buffer concentration leads to a change in the buffer capacity, hence in the surface pH, we need to consider how theses changes affect the water reduction branch of HER. The effect of pH on water reduction is opposite for Au and Pt. More accurately, the pH dependence of water reduction has been recently ascribed to a local cation concentration dependence [4]. While for Au water reduction is promoted by an increase in pH [1,4], on Pt water reduction is favoured by lower pH [15,14]. In the light of this opposite pH dependence, we tentatively interpret the bicarbonate reaction order for low buffer concentrations on Au and on Pt. Specifically, low buffer concentrations mainly result in the suppression of the pH gradient and (almost) complete consumption of the bicarbonate concentration at the surface. Accordingly, bicarbonate reduction remains unaffected by the small increase in bicarbonate concentration, and the total observed HER current is the result of the change in the surface pH on water reduction activity. Thus, starting from 2 mM, a slight increase in the bicarbonate concentration results in a lower surface pH, which inhibits water reduction on Au, but promotes it on Pt. Utilization of solutions containing high buffer concentrations minimizes the concentration gradients, hence the reaction order measured in the second regime better describes the dependence of kinetically-limited bicarbonate-mediated HER current on the bicarbonate concentration.

We investigated the effect of the cation nature on the HER in bicarbonate electrolytes. We measured voltammograms in 0.1 M $LiHCO_3/Li_2CO_3$, $NaHCO_3/Na_2CO_3$ and $KHCO_3/K_2CO_3$ on Au and Pt, as shown in Fig. 4 A and B. We reported the HER current as a function of the cation nature (C) in the less negative potential region (at −0.9 V on Au and −0.2 V on Pt) and (D) at more negative potential (-1.2 V on Au and −0.5 V on Pt). Although the measured current changes are subtle, they are consistent for three independent sets of newly prepared solutions and electrodes (see Fig. S5 and Fig. S6 in the Supporting Information). We analysed the cation dependence of the total HER measured in bicarbonate solutions, as the combination of cation effect on the two separate branches of HER. Knowing how water reduction is affected by the cation identity [5], we qualitatively subtracted this effect from the total HER current, and deduced the cation dependence of bicarbonate-mediated reduction. Considering the cation with their hydration shell, the size of hydrated alkaline cations increases in the order $K^+<Na^+<Li^+$[16]. On Au at −0.9 V, the cathodic current increases in

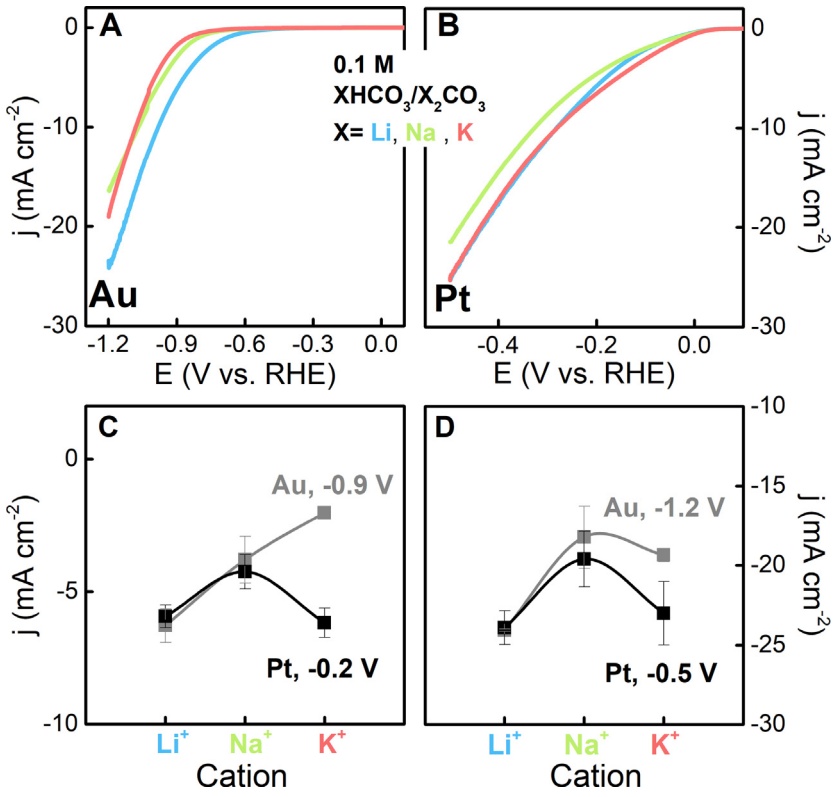

Fig. 4. Voltammetry of (A) Au and (B) Pt RDE electrode in Ar-saturated 0.1 M equimolar $XHCO_3/X_2CO_3$ with X = Li^+, Na^+ and K^+ at 10 mVs^{-1} and 2500 RPM. Dependence of the HER current on the nature of the cation at different potentials (C) Au at −0.9 V and Pt at −0.2 V and (D) Au at −1.2 V and Pt at −0.5 V.

the order K^+<Na^+<Li^+. In this potential region, we measured a reaction order of ca. 0.7 in (sodium) bicarbonate. At more negative potentials (-1.2 V), on Au the dependence of the HER current on the cation identity has changed to Li^+>K^+>Na^+. In this potential region, the measured reaction order in bicarbonate is lower (0.4), and water reduction activity impacts to a larger extent the total HER current. Water reduction on Au electrode is favoured by decreasing size of the solvated cation, i.e. K^+>Na^+>Li^+ [5]. Hence, for Au at potentials at which bicarbonate reduction is dominant, the reaction rate is promoted by larger hydrated cations (i.e. Li^+). As the potential becomes more negative, water reduction starts and the cation effect on bicarbonate reduction is counterbalanced by the cation effect on water reduction, leading to an increase in the HER for K^+ at −1.2 V. Contrary to Au, the cation effect for HER in bicarbonate on Pt is not potential dependent. The HER current is the lowest in Na^+ and larger, and comparable, for Li^+ and K^+. We again rationalize the observed trend, taking into account the cation dependence of water reduction, which on Pt is favoured by increasing size of the solvated cation [5]. It appears that on Pt, bicarbonate-mediated reduction increases in the order Li^+<Na^+<K^+. Therefore, for both electrode surfaces, we conclude that the cation effect is opposite for bicarbonate reduction *vs.* water reduction. The opposite trend of the two branches of HER would explain the minimum in the current measured for Na^+. The origin of this cation nature dependence of HER in bicarbonate may be due to the electrostatic effects on direct bicarbonate reduction [6] or to the indirect effect (of the cation dependence of water reduction) on the bicarbonate concentration gradient.

We proceeded to study the dependence of the HER current on the cation concentration. Keeping the buffer concentration constant and equal to 0.5 M, we measured voltammograms in solutions containing varying concentration of Na^+ (see Fig. S7 in the Supporting Information). Fig. 5 shows the extracted reaction order for HER in [Na^+] cation for (A) Au and (B) Pt. Increasing the cation concentration leads to a promotion of HER rate, to a different extent, on both electrodes. At less negative potentials, the reaction order in [Na^+] measured for Au (1.2) is higher than for Pt (0.5). On Au electrode the reaction order in [Na^+] gradually decreases for increasingly negative potentials, being 0.0 at the most negative applied potentials, while on Pt it is potential independent (ca. 0.5). The water reduction branch of HER at this mildly alkaline pH has been reported to be favoured by an increase in the Na^+ cation concentration on Au [4], while on Pt is unaffected (see Fig. S7 C in the Supporting Information). On Au the pH dependence of water reduction is primarily attributed to a dependence on the near-surface concentration of cation [4], and we have proposed that a similar interrelated effect between local pH and cation concentration exists also for water reduction on Pt [17]. However, for simplicity, in this work where the surface pH is additionally controlled by the buffering reactions, we refer to the direct dependence of water reduction on the near-surface cation concentration, in terms of its indirect dependence on the surface pH. Again, we attributed the potential dependence of the cation reaction order on Au, which is absent on Pt, to the different pH dependence of water reduction. Indeed, as shown in Fig. S10 (see Supporting Information), the hysteresis of the cyclic voltammograms on Au and on Pt surfaces is different. For Au, water reduction is promoted by an increase in pH, and the current in the backward scan is higher than the forward scan. Vice versa, for Pt, an increase in pH is detrimental for water reduction, and the current in the backward scan is lower than the forward scan. The hysteresis of the cyclic voltammetry on Au becomes even more pronounced in solutions containing low buffer concentrations, for which the pH gradient is steeper (see Fig. S8 Supporting Information). For the Au electrode, a promotion of water reduction is triggered by the increase in the local pH generated by bicarbonate reduction

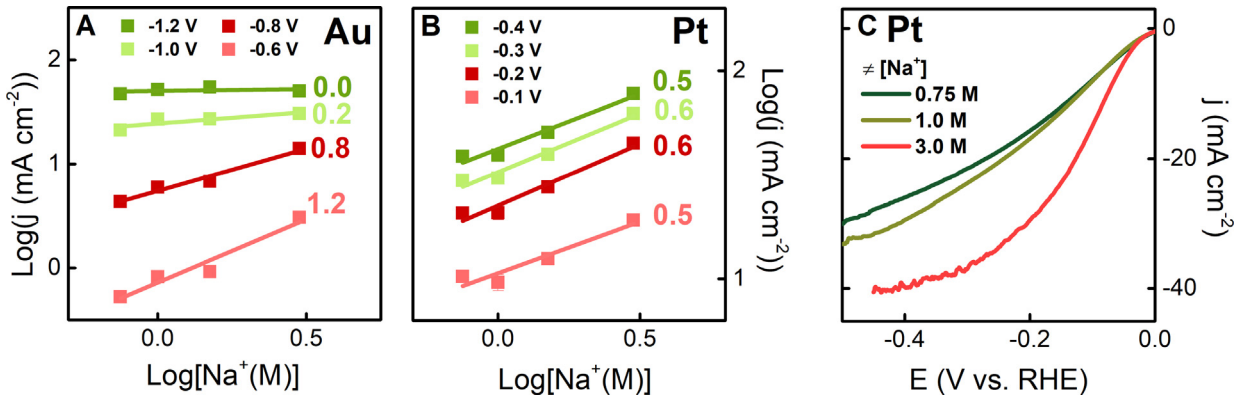

Fig. 5. Reaction order for HER in the Na^+ cation concentration at constant buffer concentration (0.5 M HCO_3^-/CO_3^{2-}) on (A) Au and (B) Pt. (C) Voltammetry of the Pt RDE electrode in Ar-saturated solutions of different Na^+ cation concentrations and constant (0.5 M) HCO_3^-/CO_3^{2-} at 10 mVs^{-1} and 400 RPM.

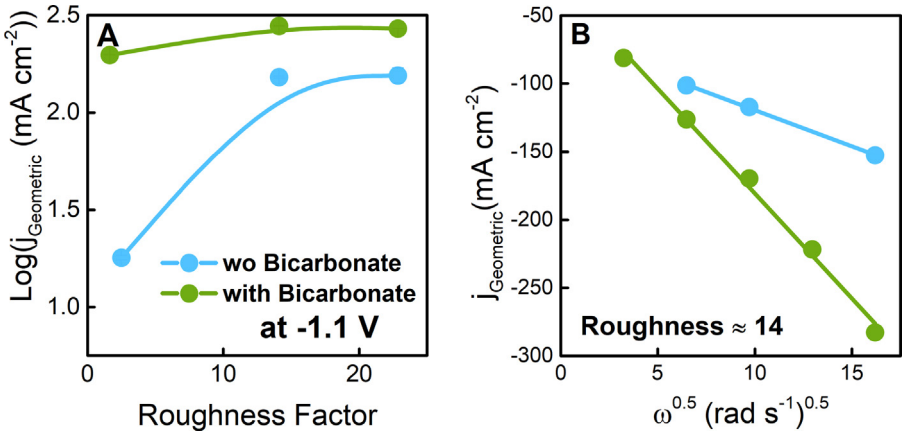

Fig. 6. (A) Dependence of the geometrical HER current on the Au electrode roughness factor, as measured at −1.1 V in bicarbonate buffer (1.0 M $NaHCO_3/Na_2CO_3$) and in perchlorate (1.5 M $NaClO_4$ + 0.1 mM NaOH) at the same pH (9.7) at 10 mVs^{-1} and 2500 RPM. (B) Dependence of the geometrical HER current on the rotation rate, as measured at −1.1 V on a Au RDE with a roughness factor of ca. 14 at 10 mVs^{-1}.

current, which in turns leads to a decrease of the bicarbonate reduction branch because of the consumption of bicarbonate by the homogeneous reactions. All together, on Au at significant negative potentials, there is strong convolution of water and bicarbonate reduction. Evaluation of the electrolyte effects on Au for bicarbonate reduction should then be carried out close to the HER onset potential, especially for low buffer concentration.

Recording voltammograms at lower rotation rate, we measured a limiting current for bicarbonate reduction on Pt, where bicarbonate reduction is less affected by the concentration gradient developed due to the concomitant promotion of water reduction with the increase in surface pH. Fig. 5 C shows the voltammograms measured for increasing Na^+ cation concentration at 400 RPM on a Pt electrode. At −0.4 V in 3.0 M Na^+, the current plateaus at a value of ca. 40 mA cm^{-2}, while the theoretical (Levich) diffusion-limited current for 0.25 M bicarbonate is 183 mA cm^{-2} [9]. The experimentally measured limiting current is therefore ca. four times lower than the one obtained for purely diffusion limitation. We may argue that this effect is in part explained as consumption of bicarbonate by the homogeneous reactions. However, this would not explain why in Fig. 5 C the limiting current also depends on the bulk concentration of Na^+, while water reduction at the same pH is independent of the cation concentration (see Fig. S7 C in the Supporting Information).

Lastly, we examined the dependence of the HER current on the electrochemically active surface area (ECSA). Generally, a mass transport-limited process scales with the geometric surface area, while a surface-limited process scales with the real surface area, i.e. the ECSA. As shown in Fig. 6 A, we measured the dependence of the geometrical HER current on the Au electrode roughness factor at −1.1 V in the presence of a bicarbonate buffer, 1.0 M $NaHCO_3/Na_2CO_3$, and in the absence, 1.5 M $NaClO_4$ + 0.1 mM NaOH, (at the same pH 9.7 and [Na^+] 1.5 M). In bicarbonate-containing electrolytes, the geometrical HER current exhibits almost no-dependence on the roughness factor. In other words, increasing the ECSA does not produces an increase in the HER current. In contrast, (in pure $NaClO_4$) water reduction displays a larger dependence on the roughness factor, with a change in the current of ca. one order of magnitude. These results suggest that, while water reduction is a surface-limited process, bicarbonate reduction is mainly controlled by mass transport. To follow up, we studied the dependence of the HER current on the rotation rate. Fig. 6 B shows the Levich plot in 1.0 M $NaHCO_3/Na_2CO_3$ and in 1.5 M $NaClO_4$ + 0.1 mM NaOH for the Au RDE with intermediate roughness factor (ca. 14). Corroborating our hypothesis, we evince a higher dependence of the HER current on the mass transport for bicarbonate reduction compared to water reduction, which is also observed for Pt electrode (see Fig. S11 in the Supporting Informa-

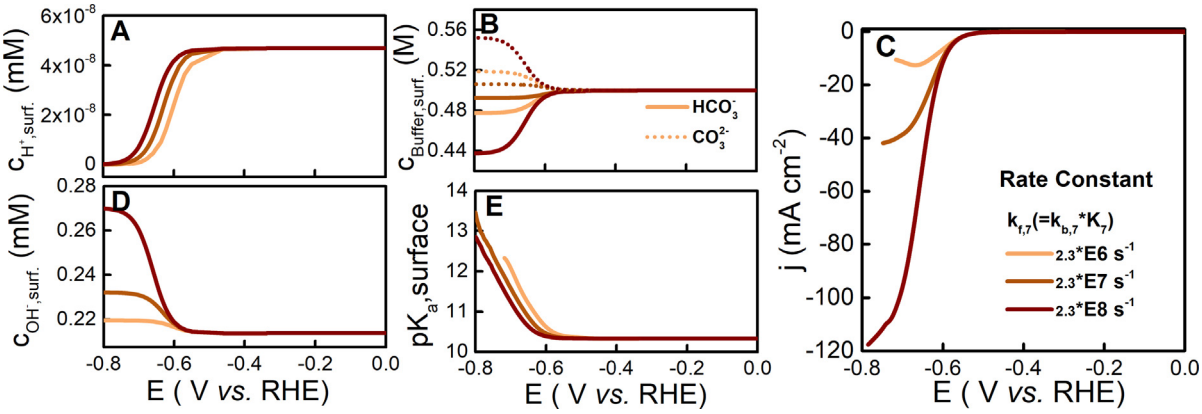

Fig. 7. Simulations of the surface concentration of (A) H^+, (B) HCO_3^- and CO_3^{2-}, (D) OH^- and (E) of the surface pK_a of reaction 7 using model I for three different values of $k_{7,f}$. (C) Simulated voltammograms for the HER current according to model I. The simulations were run at 10 mVs^{-1} and 2500 RPM in equimolar 1 M bicarbonate buffer at pH 10.33.

tion). Indeed, in the two different electrolytes, the HER current is similar at low mass transport, but is larger in bicarbonate at high mass transport rate (2500 RPM).

3.2. Microkinetic Modelling

We built a microkinetic model to establish whether bicarbonate-mediated reduction can be explained in terms of a non-electrochemical reaction in solution between water and bicarbonate that generates the hydronium ion, which then undergoes reduction (see model I in Fig. 1). The latter is the commonly accepted model to describe the role of a buffer in enhancing HER activity in acidic media [18,3]. The simulation was run using the kinetics of proton reduction on Au electrode, however as the rate of supply of the proton to be reduced depends on the kinetics of solution reactions, we may generalize the obtained conclusions to other electrode surfaces.

Fig. 7 shows the simulated surface concentrations and the HER currents according to model I for bicarbonate reduction in 1 M HCO_3^-/CO_3^{2-} employing different rate constants for reaction 7. The reported value for the rate at which bicarbonate generates a proton ($k_{7,f}$) has been derived according to $k_{7,f}=k_{7,b}*K_7=2.34$ s^{-1}, with the experimentally known value of $k_{7,b}$ and K_7 corresponding to a pK_a of 10.33 [19]. Simulations using the reported value for $k_{7,f}$ does not result in any HER current according to model I. As illustrated in Fig. 7 C, only for $k_{7,f}$ >1E6 s^{-1} the current reaches a value in the order of 10 mA cm^{-2}, which is comparable to the one obtained experimentally. From Fig. 7 A, we observe that a higher kinetics for the homogeneous reaction results in a greater ability to minimize changes in the surface concentration of proton, which is consumed at the surface following mechanism I. Since the surface concentration of H^+ is maintained by the bicarbonate buffer, as illustrated in Fig. 7B, the surface concentration of CO_3^{2-} increases for increasing values of $k_{7,f}$. Consequently, the pK_a of HCO_3^-/CO_3^{2-}, which is 10.33 in the bulk, gradually increases at the surface for more negative applied potentials (see Fig. 7E).

4. Discussion

Even if model I may work to describe the HER activity in the presence of AH in acidic media, sketching the HER activity in alkaline media in the presence of AH is less obvious. Since the concentration of free H^+ is low, to explain the experimentally observed HER current (in the order of ca. 10 mA cm^{-2}), the forward rate constant of the homogeneous reaction ($AH \rightarrow H^+ + A^-$) must be higher than 10^7 s^{-1}. This fictitious value of $k_{7,f}$ is seven orders of magnitude higher than the one reported experimentally [19]. Previous studies of HER in phosphate electrolyte postulated that the solution reactions are always at equilibrium [18,3]. However, this mechanism cannot explain the shift in onset potential observed for HER on Au on the RHE scale, for a bulk solution for which the pH is equal to the pK_a (see Fig. 2 A). It also does not explain the difference in reaction order in HER when changing the nature of the buffer (e.g. phosphate and borate) [6]. Furthermore, in model I the reactive species is the proton, and the proton reduction rate is generally independent of the cation identity and cation concentration (see Fig. S12 in the Supporting Information). Digital simulations together with the experimentally measured dependence on cation identity and concentration lead us to propose that model I is not able to explain HER in bicarbonate electrolytes.

Model II, instead, may better capture the strong dependence of HER on the cation concentration. For a given electrode material, the cation reaction order is comparable to the reaction order in bicarbonate (see Fig. 3 and 5). Notably, at less negative potentials (lower concentration gradient), we found a reaction order in HCO_3^- and Na^+ of ca. 1 on Au and ca. 0.5 on Pt. This similarity in the bicarbonate and cation dependence of HER may suggest that bicarbonate-mediated reaction mechanism involves the participation of cation. Because bicarbonate is a negatively charged species, and the surface at cathodic potential is also negatively charged, bicarbonate experiences electrostatic repulsion at reductive potentials. Using multi-scale model, Ringe et al. reported a decrease in the activity of bicarbonate at the reaction plane [20]. Thus, we expect that for increasing bulk cation concentration, the near-surface cation concentration increases, reducing the negative electrostatic repulsion experienced by the bicarbonate anion at the electrified interface. Overall, a higher near-surface cation concentration leads to an increase in the near-surface activity of the bicarbonate available for reduction to H_2, in agreement with the results observed in Fig. 5 C. According to model II, the bicarbonate reduction rate always benefits from an increase in the cation concentration, as we observed in Fig. 5. By contrast, the water reduction branch has two distinct cation concentration regimes: a promotional regime at low pH, and an inhibitive regime at higher pH [4]. This difference may be due to the different role of the cation in the mechanism of water and bicarbonate reduction. While in the first case, the cation interacts with the transition state of water dissociation step [4], in the second case, the cation may lead to an increase in the surface activity of the negatively charged reactant.

As shown in Fig. 6, bicarbonate reduction is highly dependent on mass transport, mostly because of the concentration gradient

induced by its participation in buffering reactions. Water reduction rather scales with the number of the surface active sites and exhibits a lower dependence on mass transport (for high cation concentration). Yet the interpretation of mass transport effect on water reduction branch is more complex, since it cannot be rationalized straightforward in terms of variations in the reactant concentration gradient with rotation rate. In aqueous solution, water is extremely concentrated (55.5 M) and its activity is assumed to be constant in the diffusion layer. The mass transport dependence of water reduction may be better rationalized in terms of its dependence on the near-surface cation concentration. In details, together with the current density, the rotation rate determines the local pH, as it affects the rate at which the product of water reduction, OH^-, is transported away from the surface. Following the electroneutrality principle, the change in the local pH determines the near-surface cation concentration, which may define the trend for mass transport-water reduction activity [21].

These results have important implications for CO2RR, since CO_2 is converted into bicarbonate (and carbonate) at higher pH. To achieve high selectivity for CO2RR, HER activity, both in terms of bicarbonate and water reduction, should be suppressed. In order to minimize the pH gradient, CO2RR is often performed in concentrated bicarbonate solution (0.5 M), where the bicarbonate reduction leads to an additional decrease in the selectivity towards CO2RR [2]. Various studies reported an increase in the selectivity of CO2RR for sluggish mass transport conditions, which were obtained by tuning of the electrode morphology [22,23]. The measured decrease in HER for suppressed mass transport would then reasonably be attributed to a decrease in bicarbonate-mediated reduction.

5. Conclusions

In this work, we have investigated HER in bicarbonate solutions on Pt and Au electrodes. At constant pH, a substantial improvement in the kinetics is found when bicarbonate is added in the solution. We attributed this change to an additional branch of HER, i.e. bicarbonate-mediated reduction, which becomes significant for large buffer concentrations. This reaction pathway is highly dependent on the cation concentration, most likely because of the electrostatic repulsion experienced by the negatively charged bicarbonate reactant under reductive potentials. Crucially, while water reduction has been reported to have two opposite cation-dependence regimes, bicarbonate reduction is characterized by only one cation dependence, in which a higher near-surface cation concentration is always beneficial. As elucidated with microkinetic modelling, in mildly alkaline media, the bicarbonate reduction mechanism cannot be interpreted analogously to the buffer role in acidic media, where the buffer weak acid increases the local concentration of protons, and thus promotes HER. We suggest that a more plausible mechanism involves direct bicarbonate reduction. Since bicarbonate also participates in the buffering reactions sparked by the increase in local alkalinity, an additional concentration gradient in bicarbonate is generated, justifying why bicarbonate reduction is highly dependent on mass transport. Understanding the mechanism of HER in bicarbonate electrolytes is particularly important for CO2RR electrocatalysis, since bicarbonate is ubiquitously present in CO_2-saturated solutions and the suppression of HER activity is desired.

Declaration of Competing Interest

The authors declare that they have no known competing financial interests or personal relationships that could have appeared to influence the work reported in this paper.

Acknowledgement

This project is part of the Solar-to-Products program, cofinanced by The Netherlands Organization for Scientific Research (NWO) and by ‘Shell Global Solutions International B.V’.

Appendix A. Supplementary material

Supplementary data associated with this article can be found, in the online version, at https://doi.org/10.1016/j.jcat.2021.12.012.

References

[1] A. Goyal, G. Marcandalli, V.A. Mints, M.T.M. Koper, J. Am. Chem. Soc. 142 (2020) 4154–4161.
[2] G. Marcandalli, A. Goyal, M.T.M. Koper, ACS Catalysis 11 (2021) 4936–4945.
[3] K. Obata, L. Stegenburga, K. Takanabe, The Journal of Physical Chemistry C 123 (2019) 21554–21563.
[4] A. Goyal, M.T.M. Koper, Angew. Chem. Int. Ed. 60 (2021) 13452–13462.
[5] S. Xue, B. Garlyyev, S. Watzele, Y. Liang, J. Fichtner, M.D. Pohl, A.S. Bandarenka, ChemElectroChem 5 (2018) 2326–2329.
[6] M.N. Jackson, O. Jung, H.C. Lamotte, Y. Surendranath, ACS Catalysis 9 (2019) 3737–3743.
[7] M.N. Jackson, Y. Surendranath, J. Am. Chem. Soc. 138 (2016) 3228–3234.
[8] G. Marcandalli, M. Villalba, M.T.M. Koper, Langmuir 37 (2021) 5707–5716.
[9] A.J. Bard, L.R. Faulkner, Electrochemical Methods: Fundamentals and Applications, John Wiley & Sons (2000).
[10] J. Perez, E.R. Gonzalez, H.M. Villullas, J. Phys. Chem. B 102 (1998) 10931–10935.
[11] G. Brug, M. Sluyters-Rehbach, J. Sluyters, A. Hemelin, J. Electroanal. Chem. Interfacial Electrochem. 181 (1984) 245–266.
[12] B. Conway, L. Bai, J. Electroanal. Chem. Interfacial Electrochem. 198 (1986) 149–175.
[13] T. Shinagawa, A.T. Garcia-Esparza, K. Takanabe, Scientific Reports 5 (2015) 13801.
[14] I. Ledezma-Yanez, W.D.Z. Wallace, P. Sebastian-Pascual, V. Climent, J.M. Feliu, M.T.M. Koper, Nature Energy 2 (2017) 17031.
[15] W. Sheng, Z. Zhuang, M. Gao, J. Zheng, J.G. Chen, Y. Yan, Nature Communications 6 (2015) 5848.
[16] S. Ringe, E.L. Clark, J. Resasco, A. Walton, B. Seger, A.T. Bell, K. Chan, Energy Environ. Sci. 12 (2019) 3001–3014.
[17] M.C.O. Monteiro, A. Goyal, P. Moerland, M.T.M. Koper, ACS Catalysis 11 (2021) 14328–14335.
[18] M. Auinger, I. Katsounaros, J.C. Meier, S.O. Klemm, P.U. Biedermann, A.A. Topalov, M. Rohwerder, K.J.J. Mayrhofer, Phys. Chem. Chem. Phys. 13 (2011) 16384–16394.
[19] K. Schulz, U. Riebesell, B. Rost, S. Thoms, R. Zeebe, Mar. Chem. 100 (2006) 53–65.
[20] S. Ringe, C.G. Morales-Guio, L.D. Chen, M. Fields, T.F. Jaramillo, C. Hahn, K. Chan, Nature Communications 11 (2020) 33.
[21] A. Goyal, M.T.M. Koper, J. Chem. Phys. 155 (2021) 134705.
[22] A.S. Hall, Y. Yoon, A. Wuttig, Y. Surendranath, J. Am. Chem. Soc. 137 (2015) 14834–14837.
[23] B.A. Zhang, T. Ozel, J.S. Elias, C. Costentin, D.G. Nocera, ACS Central Science 5 (2019) 1097–1105.